Computer-Aided Design of Metallopharmaceuticals: A Molecular Mechanics Force Field for Gadolinium Complexes

Thomas R. Cundari,*,†,[1] Eddie W. Moody,† and Shaun O. Sommerer‡

Departments of Chemistry, University of Memphis, Memphis, Tennessee 38152, and Barry University, Miami Shores, Florida 33161

Received February 24, 1995[⊗]

The purpose of this research is to effectively and efficiently predict the geometries of gadolinium complexes that are of a size (≈50 atoms) and which possess ligand types making them of potential interest as magnetic resonance imaging (MRI) contrast agents. This research extends a standard molecular mechanics (MM) force field for organic compounds to gadolinium complexes. Force field parameters are derived to permit modeling of prototypical hard nitrogen and oxygen ligands commonly found in lanthanide coordination chemistry. Several new ligating atom types are defined—neutral sp^3 oxygen (water, alcohols, and ethers), neutral sp^3 nitrogen (amines), neutral sp^2 oxygen (carbonyls), neutral sp^2 nitrogen (imines and pyridines), and negative oxygen (carboxylates). The new force field is generally able to predict the geometries of Gd^{III}(Schiff base)$(H_2O)_n$ and related complexes to within 3% of metric data (i.e., bond lengths and bond angles) as determined by X-ray crystallographic analysis. Torsional angles about individual bonds are also typically predicted to within 5°, allowing one to reproduce the three-dimensional (or tertiary) structure of the Gd(III) complexes. The use of a simple molecular mechanics force field permits the geometry optimization of these complexes to be carried out quickly by using commercially available software on a standard personal computer.

Introduction

Drug design is a shining example of the potential of modern computational methods to be a valuable adjunct to experiment in the search for promising lead compounds.[2,3] Computation can focus research on the most promising leads, reducing production time and costs. Computational methods have rapidly progressed for organic systems predominantly comprising a few elements from the upper right-hand corner of the periodic table.[4] Development of efficient computational methods for describing the bonding and structure of metal-containing compounds has lagged behind those for organics and is thus an active area of research.[5] Metal-containing drugs, metallopharmaceuticals, have played an important role in medicine from the use of arsenicals for the treatment of syphilis to modern uses such as technetium radiopharmaceuticals, platinum anticancer drugs, and lanthanide magnetic resonance imaging (MRI) contrast agents.[6] Technetium complexes are the most commonly used radiopharmaceuticals in medical imaging.[7] Development of cis-platin (*cis*-$PtCl_2(NH_3)_2$) and its derivatives marks a monumental advance in cancer treatment.[8] Lanthanide (Ln) complexes, in particular those of trivalent gadolinium (Gd(III)), have received great attention as MRI contrast agents.[9-17] Clearly, given the importance of metal-containing drugs and of metals in biological systems,[6,18] development and application of more efficient and effective computational approaches for such systems are needed.

Magnetic resonance imaging has quickly become the method of choice for initial screening of patients suspected of a variety of disorders.[9-17] Lauffer has analyzed the factors which yield an effective contrast agent.[9,10] The efficiency with which the contrast agent enhances proton relaxation rates in water is defined as relaxivity. Benefits of higher relaxivity include the need to use less agent (reducing cost and possible side effects) and the possibility of dynamic MRI uptake studies.[9] Since relaxivity results from interaction of water molecules in the body with a paramagnetic Gd(III) center, it is of interest to study complexes with multiple water coordination sites. A major shortcoming of GdDTPA (DTPA = diethylenetriaminepentaacetic acid) and related commercial reagents is their single water coordination site.[9] Smith et al.[13] point out that many factors determine relaxivity and that "...rational design of better MRI contrast reagents will require a more detailed understanding of the structure and dynamics of the ligand on relaxivity and

† University of Memphis.
‡ Barry University.
⊗ Abstract published in *Advance ACS Abstracts,* October 15, 1995.
(1) e-mail: cundarit@cc.memphis.edu.
(2) Sheridan, R. P.; Venkataraghavan, R. *Acc. Chem. Res.* **1987**, *20*, 322–329.
(3) Dean, P. M. *Molecular Foundations of Drug-receptor Interaction*; Cambridge University Press: Cambridge, U.K., 1987.
(4) (a) Hehre, W. J.; Radom, L.; Schleyer, P. v. R.; Pople, J. A. *Ab-Initio Molecular Orbital Theory*; Wiley: New York, 1986. (b) Cohen, N. C.; Blaney, J. M.; Humblet, C.; Gund, P.; Barry, D. C. *J. Med. Chem.* **1990**, *33*, 883–894.
(5) (a) Zerner, M. C.; Salahub, D. *The Challenge of d- and f-Electrons*; American Chemical Society: Washington, DC, 1989. (b) Cundari, T. R.; Gordon, M. S. *J. Coord. Chem.*, in press.
(6) Stadler, P. J. *Adv. Inorg. Chem.* **1991**, *36*, 1–48.
(7) Clarke, M. J.; Podbielski, L. *Coord. Chem. Rev.* **1987**, *78*, 253–331.
(8) *Platinum, Gold and other Metal Chemotherapeutic Agents*; ACS Lippard, S. J., Ed., Symposium Series 209; American Chemical Society: Washington, DC, 1983.
(9) Lauffer, R. B. *Chem. Rev.* **1987**, *87*, 901–926.
(10) Lauffer, R. B. In *Clinical Magnetic Resonance Imaging*; Edelman, R. R., Hesselink, J. R., Eds.; Saunders: Philadelphia, 1990; pp 221–236.
(11) The use of MRI contrast agents for use in imaging various portions of the body are covered in a recent special issue: *J. Magn. Reson. Imaging* **1994**, *4*, 233–510.
(12) Watson, A. D.; Rocklage, S. M.; Carvlin, M. J. In *Magnetic Resonance Imaging*; Stark, D. D., Bradley, W. G., Eds.; Mosby: St. Louis, 1992; Vol. 1, pp 372–436.
(13) Smith, P. H.; Brainard, J. R.; Morris, D. E.; Jarvinen, G. D.; Ryan, R. R. *J. Am. Chem. Soc.* **1989**, *111*, 7437–7443 and references therein.
(14) Geraldes, C. F. G. C.; Sherry, A. D.; Brown, R. D.; Koenig, S. H. *Magn. Reson. Chem.* **1986**, *3*, 242–250.
(15) Sessler, J. L.; Mody, T. D.; Hemmi, G. W.; Lynch, V. *Inorg. Chem.* **1993**, *32*, 3175–3187.
(16) Adzamli, I. K.; Gries, H.; Johnson, D.; Blau, M. *J. Med. Chem.* **1989**, *32*, 139–144.
(17) Tweedle, M. F.; Gaughan, G. T.; Hagan, J.; Wedeking, P. W.; Sibley, P.; Wilson, L. J.; Leww, D. W. *Int. J. Radiat. Appl. Instrum., Part B* **1988**, *15*, 31–36.
(18) *Progress in Inorganic Chemistry*; Lippard, S. J., Ed.; Wiley: New York, 1973, 1990; Vols. 18, 38.

0020-1669/95/1334-5989$09.00/0

stability." A combination of computation and experiment can deepen our understanding of the structure and dynamics of potential contrast agents and help assess factors which enhance relaxivity and lead to better contrast agents. To this end, we have embarked on research to develop improved computational approaches to metallopharmaceuticals. The current contribution describes our efforts to model Gd(III) complexes using molecular mechanics (MM).[19]

Brecknell et al.[20a] used MM to study Ln shift reagents; only two complexes were studied. Kemple et al.[20b] used MM to study [LaEDTA]$^-$ (EDTA = ethylenediaminetetraacetic acid) as a model for Ln−containing biomolecules; constraints are placed on Ln−ligand bond lengths due to a lack of MM parameters. Cundari used MM to analyze a Gd complex structurally characterized by Sommerer et al.[21] Lanthanide−ligand bonds were modeled using electrostatic interactions, an assumption consistent with their ionicity but entailing estimation of atomic charges (a quantum chemical property).[21] Others have also used an electrostatic Ln−ligand bonding model.[22−24] The most detailed MM study of Ln complexes is that of Hay,[25] who predicts the geometries of 57 complexes across the entire lanthanide series to within 0.03 Å and 3° of X-ray data. Although the force field is limited to two ligands (water and nitrate), it is very exciting, because of the accuracy obtained. Hay's accuracy in structural prediction (1−3%) rivals that found in more sophisticated quantum modeling of metal complexes,[5b] but with much reduced computational costs.[26]

The present research seeks to extend Hay's work to predict the structure of ligand types relevant to MRI contrast agents. The first step in computer-aided drug design is typically determination of the drug's geometry. Structures obtained with such a force field could be a starting point for other methods used to assess potential Gd(III) MRI contrast agents. Development of reliable methods for quick structure prediction is a first step in allowing the bench chemist to use computers in the design of metallopharmaceuticals.

Computational Methods

Molecular mechanics (MM) is used for all calculations described herein.[19] The molecular mechanics force field includes the terms in eq 1. The steric energy (U_{steric}) of a complex is the sum of individual bond stretching (U_r), angle bending (U_Θ), bond torsion (U_τ), and van der Waals interactions (U_{vdW}). Our driving motivation is to accurately

$$U_{steric} = \sum U_r + \sum U_\Theta + \sum U_\tau + \sum U_{vdW} \qquad (1)$$

model X-ray crystal structures of Gd complexes using a minimum of terms above and beyond the basic Allinger MM2 force field. Derivation of the present force field follows the successful precedent of Hay.[25] To simplify force-field derivation and minimize computational effort, U_r is described by a harmonic potential; thus, stretch−bend, cubic, and quartic corrections to U_r are ignored. Similarly, a harmonic potential is used for U_Θ. Torsional potentials are described using a standard, three-term Fourier series expansion. Torsional potentials are "softer" than U_r and U_Θ, particularly when a metal is involved. As a result, various researchers have set torsions about metal−ligand bonds in coordination complexes to zero,[19b] greatly reducing the number of parameters needed and leaving the minimum energy conformer to be decided primarily by nonbonded interactions. This approach was used as much as possible to yield a force field which quickly and accurately reproduces experimental data (*vide infra*). The vdW terms are calculated using a modified Buckingham potential function ($U_{vdW} = A[\exp(-Br)] - C/r^6$; A, B, and C are adjustable parameters).[19b]

The force field in Chem 3D Plus[29] differs only slightly from the MM2 force field,[19a] e.g. the option for a quartic stretching term (not used here), a cutoff distance for van der Waals interactions, and a π-orbital SCF calculation for conjugated systems.[29] A cutoff distance of 10 Å is used for van der Waals terms. For π-bonded systems the strength of a bond (hence its bond length and force constant) is modified by conjugation. A Hückel molecular orbital (HMO) calculation[30] is used to calculate π-bond orders for conjugated systems. The functional form of the π-conjugation correction used in U_r increases the force constant, and decreases the bond length, as π-bond order increases. Chem 3D Plus uses a steepest descent algorithm for geometry optimization; optimizations are carried out until the rms gradient is ≤0.010 kcal Å^{-1}. Calculations are done on either a Macintosh LC 475 or a Quadra 800.

The high coordination numbers of metal complexes have hindered application of MM to coordination complexes since numerous U_Θ(L−Ln−L) potentials must be defined.[19b] Consider a trigonal bipyramidal complex, **A**, LnL_5 (L = ligand). Even in a system as simple as LnL_5,

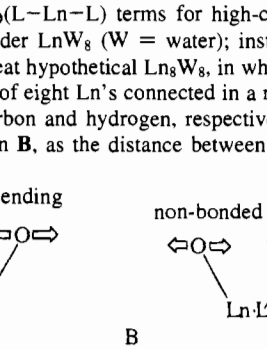

A

there are three different L−Ln−L angles (L_{eq}−Ln−L_{eq}, L_{ax}−Ln−L_{ax}, and L_{eq}−Ln−L_{ax}) each with different equilibrium angles (120, 180, and 90°, respectively) and force constants for three separate U_Θ terms. As coordination number increases and ligands are no longer the same, the number of different U_Θ terms can quickly become prohibitive.

Hay has suggested one approach for circumventing the need for a large number of U_Θ(L−Ln−L) terms for high-coordination-number complexes.[25] Consider LnW_8 (W = water); instead of treating this complex, one can treat hypothetical Ln_8W_8, in which a single water is coordinated to each of eight Ln's connected in a ring (Ln's and water are analogous to carbon and hydrogen, respectively, in cyclooctatetraene). As shown in **B**, as the distance between Ln ions in the ring

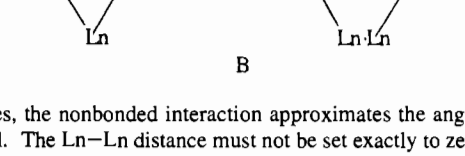

B

decreases, the nonbonded interaction approximates the angle-bending potential. The Ln−Ln distance must not be set exactly to zero to avoid overflow errors. When the Ln−Ln force constant is set very high (99 mdyn Å^{-1}) and the equilibrium Ln−Ln bond length is set to 0.001 Å

(19) (a) Allinger, N. L.; Burkert, U. Molecular Mechanics; American Chemical Society: Washington, DC, 1982. (b) Hay, B. P. *Coord. Chem. Rev.* **1993**, *126*, 177−236.
(20) (a) Brecknell, D. J.; Raber, D. J.; Ferguson, D. M. *J. Mol. Struct.* **1985**, *124*, 343−351. (b) Kemple, M. D.; Ray, B. D.; Lipkowitz, K. B.; Prendergast, F. K.; Rao, B. D. N. *J. Am. Chem. Soc.* **1988**, *110*, 8275−8287.
(21) Sommerer, S. O.; Westcott, B. L.; Krause, J.; Cundari, T. R. *Inorg. Chim. Acta* **1993**, *209*, 101−104.
(22) Fossheim, R.; Dahl, S. G. *Acta Chem. Scand.* **1990**, *44*, 698−706.
(23) Fossheim, R.; Dugstad, H.; Dahl, S. G. *J. Med. Chem.* **1991**, *34*, 819−826.
(24) Frey, S. T.; Chang, C. A.; Carvalho, J. F.; Varadarajan, A.; Schultze, L. M.; Pounds, K. L.; Horrocks, W. DeW. *Inorg. Chem.* **1994**, *33*, 2882−2889.
(25) Hay, B. P. *Inorg. Chem.* **1991**, *30*, 2876−2888.
(26) (a) Quantum chemical geometry optimization of $[Gd(OH_2)_8]^{3+}$ (S = $^7/_2$) required approximately $^1/_2$ h per optimization cycle on an IBM RS6000/25T high-performance work-station using the GAMESS quantum chemistry program package,[27] employing D_{4d} symmetry and the lanthanide effective core potentials of Cundari and Stevens.[28] (b) Molecular mechanics geometry optimization of $[Gd(OH_2)_8]^{3+}$ realized roughly three geometry optimization cycles per second on a Macintosh Quadra 800 using Chem 3D Plus software[29] and no symmetry constraints.
(27) Schmidt, M. W.; Baldridge, K. K.; Boatz, J. A.; Jensen, J. H.; Koseki, S.; Matsunaga, N. M.; Gordon, M. S.; Nguyen, K. A.; Su, S.; Windus, T. L.; Elbert, S. T. *J. Comput. Chem.* **1993**, *14*, 1347−1363.
(28) Cundari, T. R.; Stevens, W. J. *J. Chem. Phys.* **1993**, *98*, 5555−5565.

, the ring of eight Ln's collapses onto itself upon geometry optimization to give, in effect, a united Ln(III) atomic ion. The main advantage of this approach is that U_Θ(L−Ln−L) terms are effectively replaced by $U_{1,3}$(L,L) van der Waals interactions, for which parameters are readily available. Using this approach, Hay accurately reproduces geometries of 57 lanthanide aqua and nitrate complexes.[25]

In addition to the simplification which results from replacing U_Θ with $U_{1,3}$ terms for atoms with high coordination numbers, the use of $U_{1,3}$ terms is chemically satisfying, given its obvious correspondence to the highly successful "points-on-a-sphere" method of Kepert, which states that the geometry of coordination complexes is determined primarily by interactions between ligating atoms.[31] The implementation of this approach in molecular mechanics force fields has the elaboration that points (i.e., ligands) are not constrained to move on a sphere with the metal at the origin (i.e., Ln−L distances may vary).

Unlike the Allinger MM2 codes,[19a] the replacement of U_Θ(L−Ln−L) terms in eq 1 with 1,3-nonbonded (i.e. $U_{1,3}$(L--L) terms for atoms with high coordination numbers (CN ≥ 5) is a standard feature of Chem 3D Plus.[29] Hence, calculations on all $Ln(OH_2)_8^{3+}$ and $Ln(OH_2)_9^{3+}$ complexes using Chem 3D Plus yield results identical to those reported by Hay and thus remain in excellent agreement with experiment.[25,32,33]

Results and Discussion

1. Modeling of Gadolinium Complexes. Extensive research provides convincing proof of the ability of molecular mechanics to accurately predict the geometry of a large variety of organic compounds.[19] We will use the comparison of calculated and X-ray crystallographic metric data of Gd(III) complexes to evaluate the augmented force field. Solid-state structures need not be global minima. However, in order to compare theory with experiment, solid-state structures from X-ray crystallography are the only feasible alternative, given the absence of solution or gas-phase structural data for lanthanides. Clearly, any future use of force fields in computer-aided design of new structural motifs for Gd(III) MRI contrast agents will require the use of molecular dynamics, Monte Carlo, etc., techniques to probe conformational space.[2,3,4b,19] The present contribution is a first step toward this more ambitious goal. The aim is to develop a simple force field, with minimal elaborations, to quickly and effectively reproduce the structure of known Gd(III) complexes.

No geometry optimization of metal-free ligands was undertaken since geometries adopted by organic ligands upon coordination to a metal are typically very different from those found in the absence of metal. For example, the semicarbazone arms of the Schiff base DAPSC (**C**) (diacetylpyridine bis-

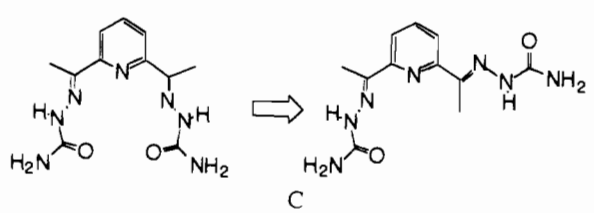

C

(semicarbazone)) come together in metal complexes to provide five ligating atoms,[21] while quantum calculations on uncomplexed DAPSC show the semicarbazone arms pointing away from each other.[34] In the next section, the ability of the augmented force field will be tested for prediction of geometries of organic ligands attached to lanthanide ions.

We are interested in ligands that have multiple coordination sites for water and form stable complexes with lanthanides.[6,9−17] Trivalent lanthanide ions show a marked preference for ligands with hard donor atoms, i.e. N- and O-donors such as carboxylates, amines, etc. Schiff bases can be constructed to incorporate N- and O-donors, and there is considerable interest in their Ln(III) complexes.[21,35] Schiff bases (R(R′)C=NR″) are formed by condensation of a primary amine (R″NH_2) and organic carbonyl (R(R′)C=O).[35,36] In addition to donor properties, Schiff bases have several properties as ligands which make them of interest as MRI contrast agents. First, Schiff bases can usually be obtained in high-yield, one-step syntheses from common starting materials.[21,35,36] Second, structural variations are simply introduced through modification of R, R′, and R″ in the starting materials.[35,36] Third, their use in oxidation catalysts, operating in harsh chemical environments, indicates that they can possess significant chemical stability.[37]

To achieve the goal of routinely studying Gd(Schiff base)-$(H_2O)_n$ and related complexes, new parameter sets must be developed which describe various types of ligated atoms. There are several new ligand types of prime importance in the present research, because these represent the typical coordinating ligands found in lanthanide chemistry and hence MRI contrast agents: neutral sp^3 nitrogen (amines), neutral sp^3 oxygen (ethers, alcohols, and water), neutral sp^2 oxygen (carbonyl) , neutral sp^2 nitrogen (imines and pyridines), and an oxygen with a negative charge (e.g., carboxylates). Prototypical ligands found in the coordination chemistry of Gd(III), and of interest in the current research, are shown in Figure 1.

The parameters needed to describe Gd complexes can be conceptually divided into two types: metal-dependent and metal-independent. A common simplification in extension of "organic" force fields to metal complexes[19b] is to assume that metal-independent parameters, derived for metal-free ligands, are transferable to coordinated ligands. For example, a C=N bond in a Schiff base is assumed to have the same force constant and equilibrium bond length whether or not the ligand is coordinated to a metal.[38,39] The prime motivation for this assumption is to minimize the effort needed in extension of an

(29) *Chem 3D Plus User's Manual*; Cambridge Scientific Computing: Cambridge, MA, 1992.
(30) Streitwieser, A. J. *Molecular Orbital Theory for Organic Chemists*; Wiley: New York, 1962.
(31) Kepert, D. L. *Inorganic Stereochemistry*; Springer: Berlin, 1982; p 31.
(32) Moody, E. W. M.S. Thesis, University of Memphis, Memphis, TN, 1994.
(33) To reproduce Hay's results, H atoms in aqua complexes were defined as atom type 5 (H attached to electroneutral atom). For the ensuing work, H atoms in aqua and alcohol ligands are defined as atom type 21 (alcohol H). The two H atom types differ slightly in their van der Waals parameters, with the latter leading to slightly less repulsive vdW interactions (to simulate the removal of electron density from H toward the electronegative O atom), and optimization of LnW_n with either H atom type leads to nearly identical results, the major difference being slightly shorter Ln−O bond lengths (≤0.03 Å).
(34) Sommerer, S. O. Unpublished results.
(35) Representative examples of Ln Schiff base complexes: (a) Backer-Dircks, J. D. J.; Gray, C. J.; Hart, F. A.; Hursthouse, M. B.; Schoop, B. C. *J. Chem. Soc., Chem. Commun.* **1979**, 774−775. (b) Bombieri, G.; Benetello, F.; Polo, A.; DeCola, L.; Smailes, D. L.; Vallarino, L. M. *Inorg. Chem.* **1986**, *25*, 1127−1133. (c) DeCola, L.; Smailes, D. L.; Vallarino, L. M. *Inorg. Chem.* **1986**, *25*, 1729−1730. (d) Guerriero, P.; Tamburini, S.; Vigato, P. A.; Benelli, C. *Inorg. Chim. Acta* **1991**, *189*, 19−27. (e) Vigato, P. A.; Fenton, D. E. *Inorg. Chim. Acta* **1987**, *139*, 39−48. (f) Bligh, S. W. A.; Choi, N.; Evagorou, E. G.; McPartlin, M.; Cummins, W. J.; Kelly, J. D. *Polyhedron* **1992**, *11*, 2571−2573.
(36) Representative syntheses of Schiff base ligands: (a) Padolik, P. A.; Jircitano, A. J.; Lin, W. K.; Alcock, N. W.; Busch, D. H. *Inorg. Chem.* **1991**, *30*, 2713−2724. (b) Sommerer, S. O.; Palenik, G. J. *Inorg. Chim. Acta* **1991**, *183*, 217−220. (c) Sommerer, S. O. Ph.D. Dissertation, The University of Florida, 1991. (d) Sommerer, S. O.; Baker, J. D.; Zerner, M. C.; Palenik, G. J. *Inorg. Chem.* **1992**, *31*, 563−567.
(37) Bailey, C. L.; Drago, R. S. *Coord. Chem. Rev.* **1987**, *79*, 321−332 and references therein.
(38) Kontoyianni, M.; Hoffman, A. J.; Bowen, J. P. *J. Comput. Chem.* **1992**, *13*, 57−65.
(39) Related papers on MM calculations on Schiff base and related complexes: (a) Klein, M.; Wingen, U.; Buss, V. *J. Am. Chem. Soc.* **1987**, *109*, 6486−642. (b) Kao, J. *J. Comput. Chem.* **1988**, *9*, 905−923.

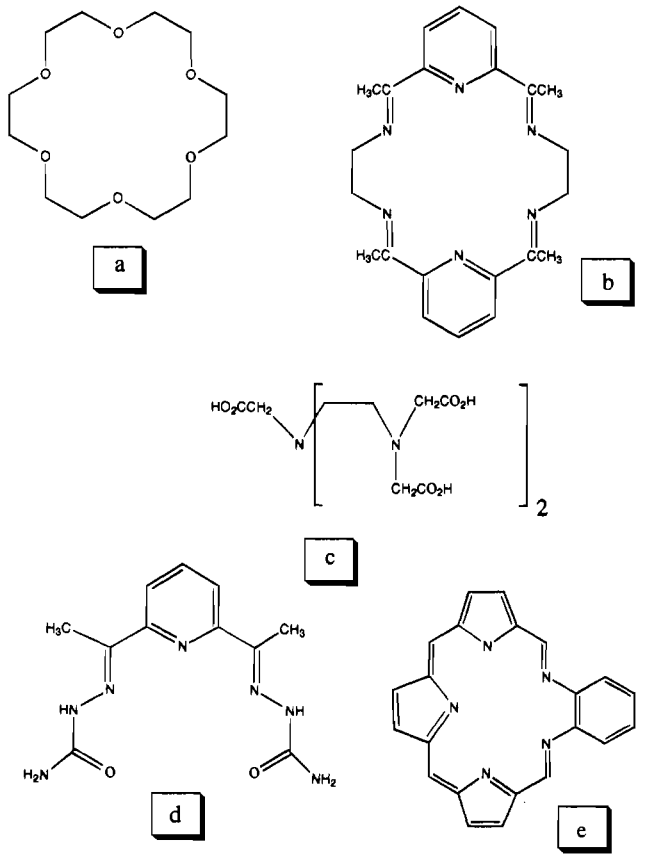

Figure 1. Prototypical ligands for Gd(III) ions: (a) 18-crown-6; (b) HAM; (c) H_5DTPA; (d) DAPSC; (e) texaphyrin.

Table 1. van der Waals Parameters for Newly Defined Ligand Types[a]

text no.	R*	eps	atom wt
	O-Coordinated Water		
85	1.740	0.050	15.995
	O-Coordinated Carboxylate		
86	1.740	0.050	15.995
	Nine-Coordinate Gd(III)		
649	3.202	0.200	157.000
	O-Coordinated Carbonyl		
807	1.740	0.066	15.995
	O-Coordinated Alkoxide		
808	1.740	0.066	15.995
	N-Coordinated Imine		
800	1.820	0.055	14.003
	N-Coordinated Amine		
888	1.820	0.055	14.003

[a] The text number is used to identify the atom type for the MM calculation;[29] R* is the van der Waals radius (Å) of the atom types. The parameter eps is given in kcal mol^{-1}. Atomic weights are reported in atomic mass units.

organic force field to Gd complexes. The assumption of transferability seems particularly reasonable in light of the ionicity of Gd−ligand bonding. However, as with all assumptions in construction of a new force field, it is necessary to test its appropriateness.

New metal-dependent and metal-independent parameters are listed in Tables 1−4. Metal-independent parameters involving new ligating atom types were taken from standard force field parameters in which the ligating atom type is replaced by a nonligating analogue. For example, the C−O equilibrium bond length and force constant for an ether linkage were used to describe a C−O bond in which O is a coordinated sp^3 oxygen (as in a crown ether complex). Exceptions to this scheme are noted below. Metal-dependent parameters needed for the study of Gd(III) complexes are derived as outlined below.

Table 2. New Bond-Stretching Parameters[a,b]

bond type	k_r	length	bond type	k_r	length
1−85	5.360	1.402	40−800	11.550	1.260
1−800	4.472	1.450	23−888	6.100	1.050
1−808	9.600	1.351	85−649	0.170	2.250
1−888	5.100	1.438	86−649	0.100	2.250
2−800	11.550	1.260	649−800	0.200	2.530
2−807	10.000	1.217	649−807	0.200	2.150
3−86	10.800	1.250	649−808	0.100	2.250
5−85	4.600	0.940	649−888	0.100	2.050
21−85	4.600	0.940			

[a] New atom type text numbers are given in Table 1. Key: 1, sp^3 C; 2, sp^2 C; 3, carbonyl C; 5, H attached to an electroneutral atom; 21, hydroxyl H; 23, amine H; 40, enamine N. Force constants (k_r) are in mdyn Å^{-1}, and bond lengths are in Å. Bond dipole = 0.00, except for the following bond types (bond dipole in parentheses): 1−85 (0.44); 1−888 (0.04); 3−86 (1.23); 23−888 (0.55). [b] Parameters needed for π-conjugation correction of new atom types (800, coordinated sp^2 N; 807, coordinated carbonyl O) were assumed to be equal to built-in parameters[29] for related noncoordinated atom types.

Table 3. New Angle-Bending Parameters[a,b]

angle type	k_Θ (mdyn Å^{-1})	XR2 (deg)	angle type	k_Θ (mdyn Å^{-1})	XR2 (deg)
1−1−85	0.70	107.500	23−40−800	0.36	113.000
1−1−800	0.45	109.470	1−85−1	0.77	106.800
1−1−808	0.38	120.000	1−85−21	0.35	106.900
1−1−888	0.57	109.470	1−85−649	0.30	125.500
3−1−888	0.90	110.300	21−85−21	0.30	109.000
5−1−85	0.54	106.700	21−85−649	0.30	120.000
5−1−800	0.50	109.471	3−86−649	0.30	125.500
5−1−888	0.50	108.800	1−800−2	0.55	118.000
1−2−800	0.55	120.000	1−800−649	0.50	120.000
1−2−807	0.38	120.000	2−800−2	0.50	120.000
2−2−800	0.43	120.000	2−800−40	0.50	120.000
5−2−800	0.35	123.600	2−800−649	0.50	120.000
7−2−40	0.50	120.000	40−800−649	0.50	120.000
40−2−40	0.50	120.000	2−807−649	0.50	120.000
40−2−807	0.50	120.000	1−808−649	0.30	125.500
1−3−86	0.43	117.000	1−888−1	0.63	107.700
7−3−86	0.80	122.000	1−888−23	0.50	109.470
3−9−37	0.50	120.000	1−888−649	0.50	109.470
2−37−9	0.50	120.000	23−888−23	0.30	109.470
1−40−800	0.43	124.000	23−888−649	0.30	109.470
2−40−800	0.43	124.000			

[a] Atom type text numbers: 1, sp^3 C; 2, sp^2 C; 3, carbonyl C; 5, H; 6, carboxyl O and enol O; 7, carbonyl O; 9, amide N; 21, alcohol H; 23, amine H; 37, pyridine N; 40, enamine N; 47, carboxylate O; 85, coordinated water O; 86, coordinated carboxylate O; 800, coordinated imine N; 807, coordinated carbonyl O; 808, coordinated alkoxide O; 888, coordinated amine N; 649, nine-coordinate gadolinium(III). [b] Out-of-plane bending force constants (for three-coordinate atoms) are 0.05 mdyn Å^{-1}, except that for type 3−86 ($C_{carbonyl}$=$O_{sp^2,coord}$), which was set to 0.80 mdyn Å^{-1}.

2. Derivation of the Force Field for Gd(III) Complexes. van der Waals Parameters. The van der Waals parameters for newly defined MM atom types are collected in Table 1. These values were estimated from standard van der Waals parameters for noncoordinated nitrogen and oxygen atom types and from the built-in parameters for lanthanum.[29]

Bond-Stretching Parameters. Newly defined MM bond-stretching parameters are collected in Table 2. Force constants and bond lengths to describe C_{alkene}=N_{imine} and N_{imine}−C_{alkane} bonds were estimated from ab-initio calculations on H_2C=N−CH_3.[40]

Equilibrium bond-stretching force constants (k_r) for Gd−ligand bonds were estimated using the values provided by Hay[25]

(40) Calculations were carried out using the GAMESS program[27] and the methods described in ref 5b.

Table 4. New Torsional Parameters[a]

torsion type	V_1	V_2	V_3	torsion type	V_1	V_2	V_3
1−1−85−649	0.400	0.520	0.467	888−1−3−86	0.000	0.000	0.000
5−1−85−649	0.000	0.000	0.530	1−1−40−23	0.000	15.000	0.000
1−1−800−649	0.000	0.000	0.000	5−1−40−1	0.000	0.000	−0.240
2−1−800−649	0.000	0.000	0.000	5−1−40−23	0.000	15.000	0.000
5−1−800−649	0.000	0.000	0.000	5−1−40−800	0.000	0.000	0.000
1−1−808−649	0.000	0.000	0.000	1−1−85−1	0.400	0.520	0.467
1−1−888−649	0.000	0.000	0.000	1−1−85−21	0.800	0.000	0.090
2−1−888−649	0.000	0.000	0.000	5−1−85−1	0.000	0.000	0.530
3−1−888−649	0.000	0.000	0.000	5−1−85−21	0.000	0.000	0.200
5−1−888−649	0.000	0.000	0.000	1−1−800−2	−0.442	0.240	0.060
1−2−800−649	0.000	0.000	0.000	2−1−800−2	0.100	0.000	0.500
2−2−800−649	0.000	15.000	0.000	5−1−800−2	0.000	0.000	−0.240
5−2−800−649	0.000	0.000	0.000	1−1−888−1	−0.200	0.730	0.800
1−2−807−649	0.000	15.000	0.000	1−1−888−23	0.000	0.120	0.100
40−2−807−649	0.000	15.000	0.000	2−1−888−1	0.000	0.000	0.000
80−2−807−649	0.000	0.000	0.000	3−1−888−1	0.000	0.000	0.000
1−3−86−649	−3.290	5.600	0.000	5−1−888−1	0.000	0.000	0.520
7−3−86−649	−3.290	5.600	0.000	5−1−888−23	0.000	0.000	0.250
1−40−800−649	0.000	0.000	0.000	1−2−2−800	−0.270	10.000	0.000
2−40−800−649	0.000	15.000	0.000	2−2−2−800	−0.930	8.000	0.000
5−40−800−649	0.000	0.000	0.000	5−2−2−800	0.000	9.000	−1.060
23−40−800−649	0.000	15.000	0.000	800−2−2−800	−0.930	8.000	0.000
1−1−1−85	0.100	0.100	0.180	1−2−40−1	0.000	10.000	0.000
1−1−1−800	0.100	0.400	0.500	1−2−40−800	0.000	15.000	0.000
1−1−1−888	0.100	0.400	0.500	40−2−40−1	0.000	15.000	0.000
2−1−1−808	0.000	0.000	0.180	40−2−40−5	0.000	15.000	0.000
5−1−1−85	0.000	0.000	0.180	40−2−40−23	0.000	15.000	0.000
5−1−1−800	0.000	0.000	0.500	40−2−40−800	0.000	15.000	0.000
5−1−1−808	0.000	0.000	0.180	807−2−40−1	0.000	0.000	0.000
5−1−1−888	−0.150	0.000	0.150	807−2−40−5	0.000	15.000	0.000
11−1−1−808	0.000	−1.400	0.180	807−2−40−23	0.000	15.000	0.000
85−1−1−85	0.000	−0.600	0.300	807−2−40−800	0.000	0.000	0.000
85−1−1−888	0.000	−0.600	0.300	1−2−800−1	0.000	10.000	0.000
800−1−1−800	2.100	0.027	0.093	1−2−800−2	−0.270	10.000	0.000
888−1−1−888	0.000	0.000	0.000	1−2−800−40	0.000	10.000	0.000
1−1−2−800	0.000	0.000	0.000	2−2−800−1	−0.270	10.000	0.000
1−1−2−807	−0.440	0.240	0.060	2−2−800−2	−0.930	8.000	0.000
5−1−2−86	0.000	0.000	0.000	2−2−800−40	0.000	10.000	0.000
5−1−2−800	0.000	0.000	0.000	5−2−800−1	0.000	12.500	0.000
5−1−2−807	0.000	0.000	0.200	5−2−800−2	0.000	9.000	−1.060
800−1−2−40	0.000	0.000	0.600	1−40−800−2	0.000	0.000	0.000
800−1−2−807	0.000	0.000	0.000	2−40−800−2	0.000	0.000	0.000
888−1−2−40	0.000	0.000	0.600	5−40−800−2	0.000	15.000	0.000
888−1−2−86	0.000	0.000	0.000	23−40−800−2	0.000	15.000	0.000
888−1−2−807	0.000	0.000	0.000	1−85−649−85	−0.170	−1.200	0.000
5−1−3−86	0.000	0.000	0.000	1−85−649−888	−0.170	−1.200	0.000
888−1−3−7	0.000	0.000	0.000				

[a] V_1, V_2, and V_3 are the 1-, 2-, and 3-fold barriers for rotation about a particular bond. For an arbitrary dihedral of type i−j−k−l, the paramters describe rotation about the j−k bond. All X−Y−649−Z torsions have been set to $V_1 = V_2 = V_3 = 0.000$, except those noted above. Atom types: 1, sp^3 C; 2, sp^2 C; 3, carbonyl C; 5, H attached to electroneutral atom; 7, carbonyl O; 9, amide N; 21, alcohol H; 23, amine H; 28, enol H; 37, pyridine N; 40, pyrrole N; 85, coordinated water O; 86, coordinated carboxylate O; 649, nine-coordinate gadolinium; 800, coordinated imine N; 807, coordinated carbonyl O; 808, coordinated alkoxide O; 888, coordinated amine N.

for Gd−O_{aqua} as a starting guess. In general, k_r fall in the range 0.1−0.2 mdyn Å^{-1} for Gd−ligand bond lengths. As a comparison, the k_r for a C_{alkane}−C_{alkane} bond is 4.4 mdyn Å^{-1}.[29] Equilibrium bond lengths were obtained in the following fashion. Inspection of r_0 values for Hay's MM study of Ln(H_2O) complexes shows them to be ≈0.2−0.3 Å *shorter* than bond lengths measured in X-ray diffraction studies of model complexes.[25] A very small k_r allows the Gd−ligand bonds substantial flexibility in terms of expanding (or contracting) to accommodate changes such as the size of the central Gd(III) ion and constriction brought about as a consequence of chelation of the ligand to the metal. Such a "soft" description of the Gd−ligand interaction is needed to allow the bonds to expand or contract in response to bonding forces elsewhere in the ligand. In X-ray structural analyses of lanthanide complexes, it is not unusual to see Ln−ligand bonds of the same type vary by ≥0.1 Å.[13,15,21,25,34,35] In developing parameters for the five new coordination bond types (Gd−O_{sp^2}, Gd−O_{sp^3}, Gd−N_{sp^2}, Gd−N_{sp^3}, and Gd−O^-), we found this approach to be successful.

Angle-Bending Parameters. There are two types of metal-dependent angle-bending parameters, X−Gd−Y and Gd−X−Y. As described above, X−Gd−Y angle-bending terms are replaced with 1,3-nonbonded repulsion terms ($U_{1,3}$(X,Y)). The only parameters needed for the $U_{1,3}$ approach are the vdW parameters described above. To describe the Gd−X−Y angle-bending potential, we have chosen equilibrium bond lengths taken from X-ray crystallographic data of the calibration complexes discussed below. The angle-bending force constants were chosen to be consistent with that employed by Hay[25] for describing Ln−O−H bending in aqua complexes, i.e. $k_\Theta = 0.3$ mdyn Å^{-1}. In some cases a harder Gd−X−Y bending potential was used ($k_\Theta = 0.5$ mdyn Å^{-1}) to give better agreement with experimental structures. New angle-bending parameters are collected in Table 3.

Torsional Parameters. There are two types of metal-dependent torsions: X−Y−Z−Gd and X−Y−Gd−Z. The latter describe rotation about the Gd−ligand bonds and can be set to zero with a good degree of confidence because the large

r_0 and ionicity of Ln−ligand bonds suggest small, if any, barriers to rotation. Such an approach has been used extensively in previous molecular mechanics applications to metal complexes[19b] and found to provide an economical description of rotation about metal−ligand bonds with minimal effort (since such torsions tend to be the majority of missing parameters in MM force field extensions to metal complexes). Somewhat more speculative is the assumption of zero rotational barriers for the former torsion type, i.e. X−Y−Z−Gd. In general, this assumption has been made to describe the small torsional barriers about single bonds, e.g. C_{alkane}−X bonds where X is a coordinated sp^3 nitrogen or oxygen. Various researchers have used the assumption of modeling X−Y−Z−Gd parameters with X−Y−Z−C_{alkane} torsional parameters. We have used this approximation where doing so led to considerable improvement in the reproduction of X-ray structures. The use of barrierless metal-dependent torsions means that the overall three-dimensional (i.e., tertiary) structure of the Gd complexes will be primarily determined by nonbonding interactions among the ligands and the structural requirements of their chelation to the metal. The assumption seems particularly appropriate for lanthanide complexes since the ionic lanthanide−ligand bonds are highly ionic and hence nondirectional. As before, the desire to ease the task of developing a MM force field and minimize calculation times is another important motivating factor for this simplification.

Given the similarity of the bonding across the lanthanide series, we expect that parameters for Ln complexes to the left and right of Gd(III) could easily be obtained with little additional effort. Since Gd is of prime importance in MRI contrast agent design, we concentrated our efforts on reproducing the structure of Gd complexes.

3. Application of the Force Field to Gd(III) Complexes. With derivation of a molecular mechanics force field as outlined above, it is now possible to apply it to a wide variety of complexes. Representative complexes, incorporating typical ligand motifs (Figure 1) encountered in contrast agents, used for validation of the force field are described below. Geometry optimizations were started from X-ray coordinates; ancillary ligands other than water were replaced with aqua ligands. Systems studied with the newly derived MM force field include $[Gd(texaphyrin)(H_2O)_4]^{2+}$ (**1**), $[Gd(DAPSC)(H_2O)_4]^{3+}$ (**2**), $[Gd(Kyptofix)(H_2O)]^{3+}$ (**3**), $[Gd(tetraethylene\ glycol)(H_2O)_4]^{3+}$ (**4**), $[Gd(C_{28}H_{28}F_{24}O_4N_4)_2]^{+}$ (**5**), $[Gd(18\text{-}crown\text{-}6)(H_2O)_3]^{3+}$ (**6**), $[Gd(HAM)(H_2O)_4]^{3+}$ (**7**), $[Gd(EDTA)(H_2O)_3]^{-}$ (**8**), and $[Gd(tren)_2(H_2O)]^{3+}$ (**9**).[41] Analogues of **3**, **5**, and **9** have been reported with Eu(III),[42] Ce(IV),[43] and Nd(III)[44] as the central lanthanide ion. In these cases, agreement between theory and experiment is good once consideration is taken of the differing ionic radii of lanthanide ions.[32] All bond lengths and bond angles involving main group atoms on ligands show good agreement with experimental data as expected for molecular mechanics when applied to organic systems.[19,32] It will be seen below that metric parameters involving the lanthanide are predicted as accurately as metal-independent metric parameters. A more in-depth analysis is presented below for structurally characterized Gd complexes (**1**, **2**, **4**, **6**, **7**, and **8**) incorporating ligand motifs commonly found in MRI contrast agents.

(41) tren = triethylenetetramine; Kryptofix = 4,7,13,16,21,24-hexaoxa-1,10-diazabicyclo[8.8.8]hexacosane; $C_{28}H_{28}F_{24}O_4N_4$ = bis[1,1,1,12,-12,12-hexafluoro-2,10-bis(trifluoromethyl)-4,9-dimethyl-5,8-diazadodeca-4,8-diene-2,11-diolato(2−)].

(42) Ciampolini, M.; Dapporto, P.; Nardi, N. *J. Chem. Soc., Chem. Commun.* **1978**, 788−789.

(43) Timmons, J. H.; Martin, J. W. L.; Martell, A. E.; Rudolf, P.; Clearfield, A.; Arner, J. H.; Loeb, S. J.; Willis, C. J. *Inorg. Chem.* **1980**, *19*, 3553−3557.

(44) Eigenbrot, C. W.; Raymond, K. N. *Inorg. Chem.* **1982**, *21*, 2867−2870.

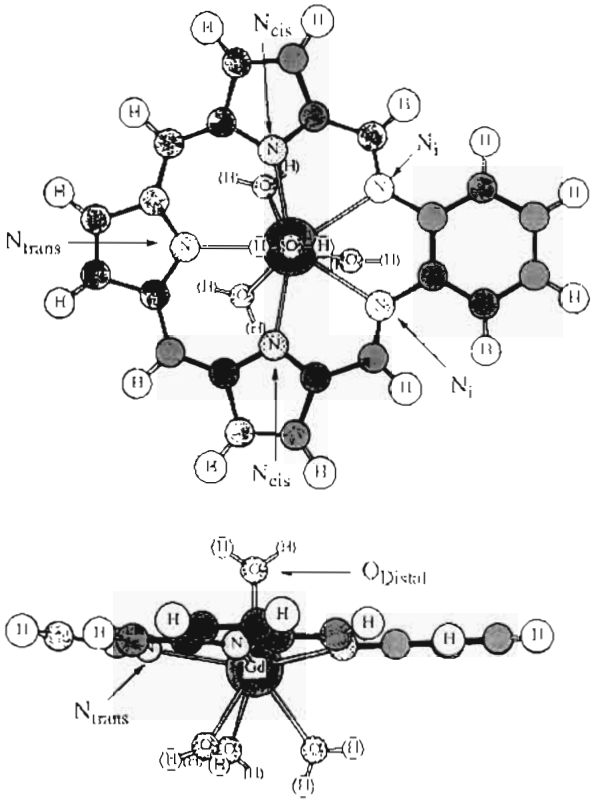

Figure 2. Top: MM-optimized $[Gd(texaphyrin)(H_2O)_4]^{2+}$ complex viewed along the bond axis connecting Gd(III) and the oxygen of the single distal water. Bottom: View perpendicular to this axis.

$[Gd(texaphyrin)(H_2O)_4]^{2+}$, 1. Two Gd−texaphyrin complexes have been structurally characterized (see Figure 1 for the parent texaphyrin ligand), differing only in substituents on the texaphyrin macrocycle;[15] average Gd−N bond lengths, as determined by X-ray diffraction, for five ligated nitrogens are 2.49 ± 0.08 and 2.46 ± 0.07 Å. The MM force field accurately reproduces these bond lengths quite well; Gd−N = 2.52 ± 0.09 Å, average differences of 1−2%. The new force field also accurately reproduces subtle trends in Gd−N bond lengths. For experimentally characterized Gd(texaphyrin) complexes and the MM model, Gd−N bond lengths are in the order Gd−N_i > Gd−N_{trans} > Gd−N_{cis}; see Figure 2. Ligand-Gd−ligand angles involving the macrocycle are very accurately predicted for pyrrole (N_{trans} and N_{cis}) and imine (N_i) nitrogens: N_i−Gd−N_i = 64° (62.0(2) and 63.7(1)°)); N_{trans}−Gd−N_{cis} = 78° (75.4(1) and 75.6(1)°); N_i−Gd−N_{cis} = 66° (65.5(1) and 66.4(9)°). The average difference in bond lengths between theory and experiment is 0.03 Å for one Gd(texaphyrin) and 0.02 Å for the other. The MM-calculated structure differs from the experimental structures by an average between 2 and 3° for all bond angles, as well as for X−Gd−Y and Gd−X−Y bond angles. Torsional angles are also well reproduced by the new force field, showing an average difference of 5−6°. Torsional angles involving the metal (Gd−X−Y−Z and X−Gd−Y−Z) are only slightly less well reproduced with the average differences between MM and X-ray being 1−2° higher than the average difference for all torsions. An overlay of calculated **1** and one of the Gd−texaphyrin complexes (complex **37** in ref 15), Figure 3, shows good agreement in the tertiary structure of the MM and X-ray structures. The buckling of the texaphyrin caused by the out-of-plane Gd(III) (*vide infra*) is seen in both calculated and experimental structures.

The O-bonded ligands in the experimentally characterized Gd−texaphyrin complexes are bidentate nitrates and thus are not comparable to the aqua ligand used in the model. However, the average calculated Gd−OH_2 bond length is 2.44 Å for **1**, a

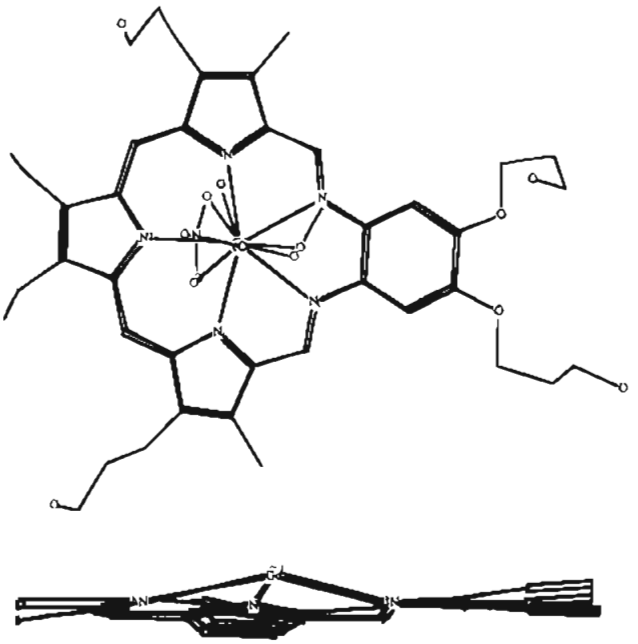

Figure 3. Overlay of MM-calculated structure of $[Gd(texaphyrin)(OH_2)_4]^{2+}$ and X-ray crystallographic structure of the Gd(III) complex of 4,5-diethyl-10,23-dimethyl-9,24-bis(3-hydroxypropyl)-16,17-bis((3-hydroxypropyl)oxy)-13,20,25,26,27-pentaazapentacyclo[20.2.1.1^{3,6}.1^{8,11}.0^{14,19}]heptacosa-3,5,8,10,12,14,16,18,20,22,24-undecaene. The unit cell also has two nitrate counterions plus water and methanol.

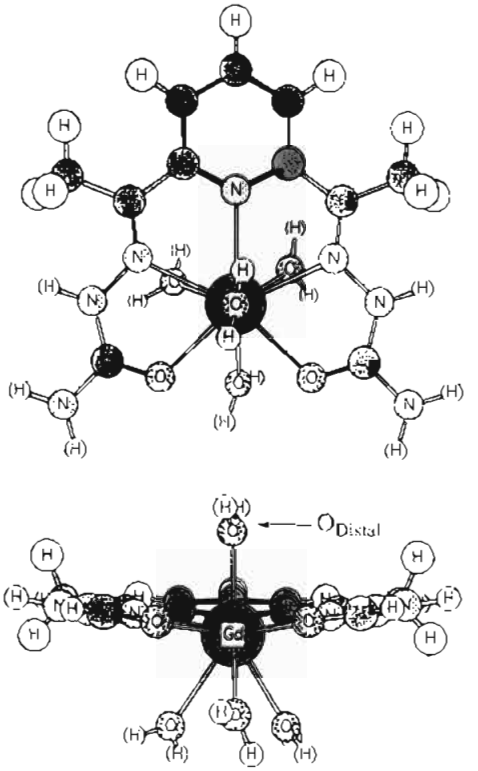

Figure 4. Top: View of MM-optimized $[Gd(DAPSC)(OH_2)]^{3+}$ along the bond axis connecting Gd and the distal oxygen. Bottom: View along an axis normal to the top view.

value consistent with the average experimental Gd−OH_2 bond lengths in three $[Gd(H_2O)_9]^{3+}$ complexes (differing only in the counterions) of 2.45, 2.45, and 2.44 Å.[25]

An additional point of interest concerning the geometry of **1** revolves around the position of Gd relative to the N_5 plane. In the experimental systems Gd is significantly out of the N_5 plane, 0.6−0.7 Å depending on texaphyrin substituents.[15] The four aqua ligands in **1** are distributed such that three are on one face of the texaphyrin with the fourth coordinated to the opposite face (Figure 2), an arrangement which gives the GdW_4 moiety in **1** a distorted tetrahedral geometry. In complex **1** Gd(III) is 0.5 Å out of the texaphyrin N_5 plane (toward the side with three coordinated waters), in good agreement, despite the difference in axial ligands, with the experimental (nitrate) systems. Sessler et al.[15] propose that, with a symmetrical axial ligand environment, Gd(III) can fit in the texaphyrin cavity and thus be coplanar with the N_5 plane. To investigate this hypothesis, we investigated an isomer of **1** in which two waters are coordinated to Gd on both sides of the macrocycle. Upon MM minimization, the latter symmetrical isomer possesses a nearly perfectly planar Gd(texaphyrin) moiety; i.e., Gd(III) is coplanar with the N_5 plane of the texaphyrin. Thus, MM calculations support the experimental hypothesis[15] and show that ancillary aqua ligands have a profound effect on the geometry of the macrocycle and hence the geometry of the resulting complex.

$[Gd(DAPSC)(H_2O)_4]^{3+}$, 2. Sommerer et al.[21] have synthesized and structurally characterized $[Gd(DAPSC)(H_2O)_4][NO_3]_3$ (Figure 4). Agreement between the MM-optimized structure and X-ray diffraction data is excellent and is superior to a previous MM description of **2** in which Gd(III)−ligand interactions were described using an electrostatic bonding model.[21] The average differences in heavy-atom bond lengths between MM and X-ray data are 0.03 Å (all bonds) and 0.06 Å (for the nine Gd−L bonds), an average deviation of only 2.5% in both cases. Bond lengths, angles, and torsions involving hydrogens are not included in structural analyses, since the positions of hydrogen atoms are not often accurately determined in X-ray diffraction experiments. The average absolute difference between the MM geometry and the X-ray structure of **2** is 4° for all angles involving heavy atoms. The average absolute differences between theory and experiment for X−Gd−Y and Gd−X−Y angles are 4 and 3°, respectively. The newly derived force field shows the ability to predict even the softest (and hence most difficult to accurately model) potentials—torsions. The ability to model torsions is important, since they determine the tertiary structure of a complex. The average difference between experimental and calculated torsions is only 5°. Agreement between MM and X-ray is similarly good for X−Gd−Y−Z (average difference = 6°) and Gd−X−Y−Z (average difference = 4°), supporting the use of the simplifying assumptions discussed above for these torsional parameters.

Complexes **1** and **2** show interesting similarities; both are nine-coordinate complexes comprising a near-planar pentadentate ligand and a pseudotetrahedral GdW_4 (W = OH_2) moiety. As with texaphyrin, it is of interest to assess the geometry of $[Gd(DAPSC)]^{3+}$ in the absence of coordinated water. Removal of the four water molecules from MM-optimized $[Gd(DAPSC)(H_2O)_4]^{3+}$, followed by further geometry optimization, results in a perfectly planar complex. Of course, one should exercise care in applying Gd(III) parameters (developed for high-coordination complexes) to a five-coordinate model. However, as with texaphyrin, DAPSC is a conjugated system with great sensitivity in its tertiary structure to the remaining ligand environment. Synthetic and computational studies are under way in our laboratory to see how the coordination geometries of lanthanide complexes change as the DAPSC ligand is functionalized.

$[Gd(tetraethylene\ glycol)(H_2O)_4]^{3+}$, 4. Rogers et al. have structurally characterized $[Gd(Cl)(OH_2)_3(EO_4)]Cl_2 \cdot H_2O$, EO_4 = tetraethylene glycol.[45] The coordinated chloride is replaced with an aqua ligand to yield the model $[Gd(OH_2)_4](tetraethylene\ glycol)]^{3+}$ which was submitted to MM study, Figure 5. Complex **4** is of particular interest since it possess three different types of neutral sp^3 oxygen ligand types (coordinated water, ether, and alcohol) in two different coordination sites (prismatic

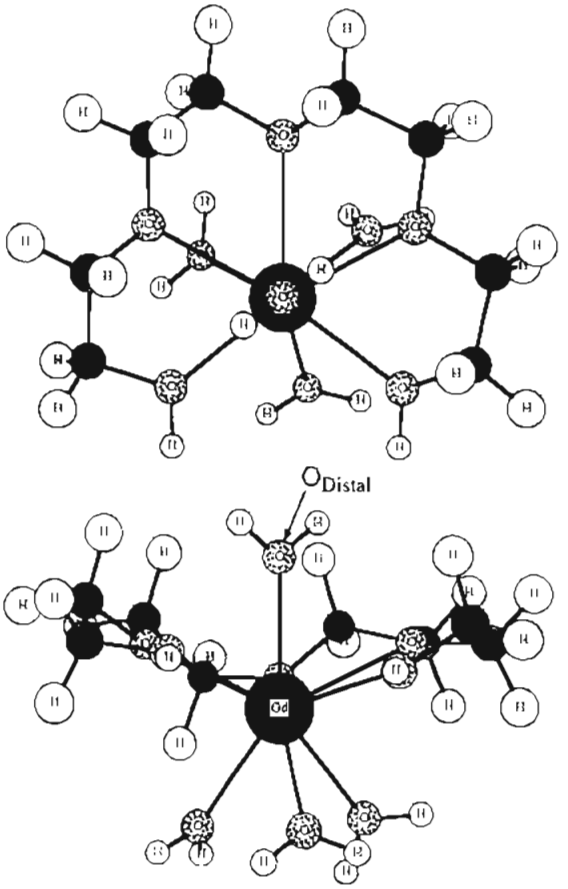

Figure 5. Top: MM-optimized structure of [Gd(tetraethylene glycol)-$(OH_2)_4$]$^{3+}$ viewed along the axis connecting Gd and the oxygen of the distal water. Bottom: View normal to this axis.

and capping). The Gd−O bond lengths for water ligands in capping and prismatic coordination sites are 2.45 Å (MM, 2.495-(4) Å, experimental) and 2.40 Å (MM, 2.41(3) Å, experimental) for the tricapped trigonal prism structure. As shown in **D**, MM-

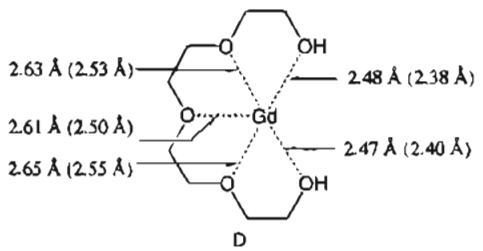

D

calculated Gd−O bond lengths are roughly 0.1 Å longer than observed although trends in relative Gd−O bond lengths are very accurately reproduced. This corresponds to an average difference in bond lengths of ≈3% for all Gd−O bonds, as compared to 2% (0.04 Å) for all bonds in the EO_4 complex. The average differences between the MM and X-ray data are 3° for all bond angles, 4° for X−Gd−Y angles, and 4° for Gd−X−Y angles for the [Gd(EO_4)]$^{3+}$ moiety. Calculated torsional angles differ by ≈7° for metal-independent and metal-independent torsions.

The EO_4 ligand in **4**, like those in **1** and **2**, is pentadentate, forming a pseudotetrahedral arrangement with a GdW_4 moiety. As for **1** and **2**, it is of interest to see what changes in the Gd-(EO_4) unit take place upon removal of the four aqua ligands. Starting with MM-optimized **4**, removing four water molecules, followed by geometry optimization, shows the [Gd(EO_4)]$^{3+}$ moiety of the anhydrous complex to be nearly identical to that in **4**. Unlike texaphyrin and DAPSC, EO_4 is not a conjugated

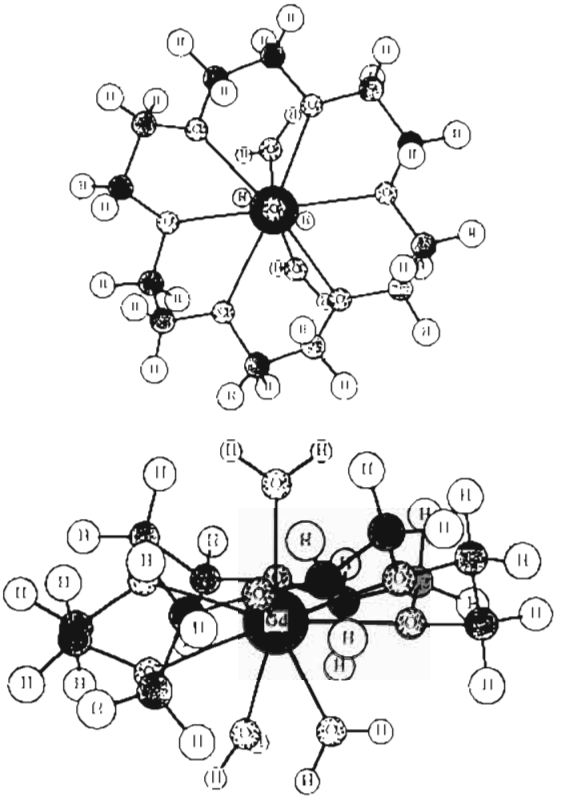

Figure 6. MM-optimized [Gd(18-crown-6)$(OH_2)_4$]$^{3+}$: (top) view along Gd−O axis, normal to best-fit plane described by six ether oxygens; (bottom) view normal to this axis.

π system, so that removal of the four aqua ligands provides little driving force for geometric distortion.

[Gd(18-crown-6)$(H_2O)_3$]$^{3+}$, 6. Rogers et al. have structurally characterized [Gd(Cl)$(OH_2)_2$(18-crown-6)]$Cl_2 \cdot 2H_2O$ and [$GdCl_6$]-[$GdCl_2(OH_2)$(18-crown-6)][$GdCl(OH_2)_2$(18-crown-6)]·2OHMe; the former has a disorder in one of the ethylene units, and so our analysis focused on the latter complex.[46] The inner coordination sphere chlorides are replaced with aqua ligands, and the resulting [Gd(18-crown-6)$(H_2O)_3$]$^{3+}$ complex geometry is optimized; see Figure 6. Agreement between the MM-optimized structure and X-ray diffraction data is good. The average differences in bond lengths between MM and X-ray data are 0.04 Å for all bonds and only 0.08 Å for the Gd−L bonds, average differences of less than 3%. The average differences between MM and X-ray are 4° (<5%) for all angles, 4° for angles about Gd(III) (i.e., X−Gd−Y), and 4° for Gd−X−Y angles. The average differences between MM and X-ray torsions are 7° for all torsions, 7° for torsions about Gd−ligand bonds, and 4° for Gd−X−Y−Z torsions.

Hay and co-workers have extensively investigated, and obtained excellent results with, MM for modeling crown ether complexes of alkali metal and alkaline earth metal cations.[47] One complication in the present work is the use of the same atom type for all coordinated sp^3 oxygens, whether they are ethers, alcohols, or water. One could circumvent this by defining a new atom type to distinguish between coordinated waters and coordinated ethers (or alcohols), but this entails a commensurate increase in the parametrization effort. Given the

(45) Rogers, R. D.; Etzenhouser, R. D.; Murdoch, J. S.; Reyes, E. *Inorg. Chem.* **1991**, *30*, 1445−1455.
(46) (a) Rogers, R. D.; Kurihara, K. K. *Inorg. Chem.* **1987**, *26*, 1498−1502. (b) Rogers, R. D.; Rollins, A. N.; Etzenhouser, R. D.; Voss, E. J.; Bauer, C. B. *Inorg. Chem.* **1993**, *32*, 3451−3462.
(47) (a) Hay, B. P.; Rustad, J. R. *J. Am. Chem. Soc.* **1994**, *116*, 6316−6326. (b) Hay, B. P.; Rustad, J. R.; Hostetler, C. J. *J. Am. Chem. Soc.* **1993**, *115*, 11158−11164.

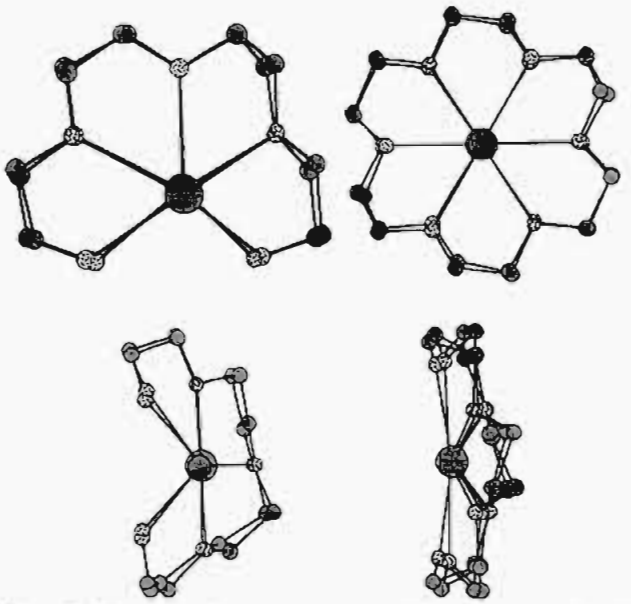

Figure 7. Overlays of MM-optimized and X-ray structures for Gd polyether complexes of tetraethylene glycol (left-hand side) and 18-crown-6 (right-hand side). H atoms have been omitted for clarity.

similarity in the bonding of the lanthanides and the larger alkali metal and alkaline earth metal cations (e.g., the preference for large coordination numbers and the highly ionic bonding), it should be possible to further refine a force field to improve the agreement between theory and experiment for lanthanide crown ether complexes. Comparing the data for the acyclic (EO_4) and macrocyclic (18-crown-6) Gd(III) complexes shows similar good agreement between theory and experiment. Overlays of the calculated and experimental structures for the $[Gd(EO_4)]^{3+}$ and $[Gd(18\text{-crown-}6)]^{3+}$ fragments of **4** and **6** are shown in Figure 7.

$Gd(HAM)(H_2O)_4]^{3+}$, 7. The next complex studied, $[Gd(HAM)(H_2O)_4]^{3+}$ (**7**; see Figure 8), does not have an exact experimental analogue, since acetates are coordinated in a bidentate fashion in the X-ray structure of $[Gd(HAM)(acetate)_2]Cl\cdot 4H_2O$.[13] It is interesting to note that $[Gd(HAM)(acetate)_2]Cl\cdot 4H_2O$, like the texaphyrin complexes (*vide supra*), does not have inner coordination sphere water in the solid state, despite the fact that their syntheses are performed in aqueous media. Note that the DAPSC complex has four inner coordination sphere aqua ligands, unlike Gd HAM and texaphyrin complexes, suggesting that DAPSC provides a hydrophilic pocket which does not exclude water. Although both inner and outer sphere waters play a role in lanthanide-induced relaxation,[9] the strengths of these interactions are inversely proportional to the sixth power of the $Gd-H_{aqua}$ distance, making it desirable to have water protons as close as possible to the paramagnetic Gd(III) center. This raises the question of whether or not large hydrocarbon ligands such as HAM[13] and texaphyrins[15] create a hydrophobic pocket that excludes water, while a more polar ligand such as DAPSC[21] creates a hydrophilic pocket and facilitates water coordination.

Agreement in pertinent metric data (i.e., within the $[Gd(HAM)]^{3+}$ moiety) for **7** and $[Gd(HAM)(acetate)_2]Cl\cdot 4H_2O$ is excellent. The average differences between theory and experiment are 0.02 Å (1%) for all bond lengths (36 bond lengths), 0.07 Å (3%) for six Gd−N bond lengths, 2° (2%) for all 67 bond angles, 2° for 15 N_1-Gd-N_2 angles, 1° for 12 Gd−X−Y angles, 6° for all 130 dihedrals, 8° for 20 Gd−X−Y−Z dihedrals, and 5° for 60 X−Gd−Y−Z dihedrals. An overlay of the MM and X-ray structures for the $[Gd(HAM)]^{3+}$ moiety is given in Figure 9.

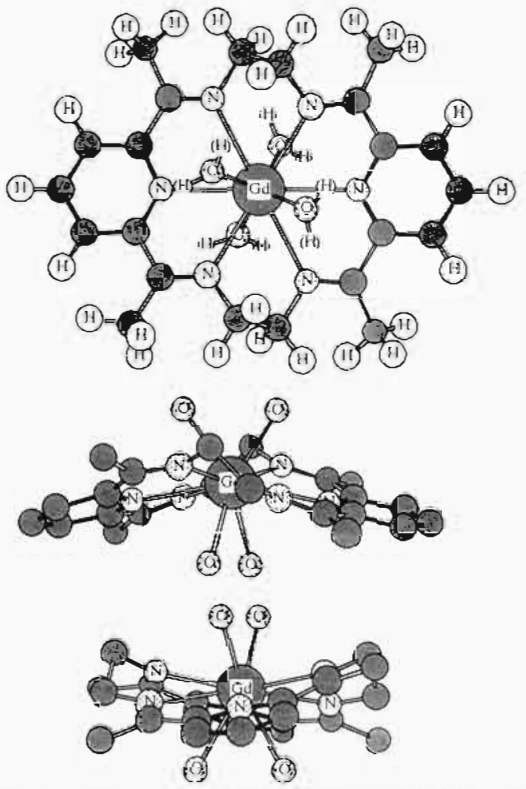

Figure 8. Different views of MM-optimized $[Gd(HAM)(OH_2)_4]^{3+}$ (**7**). In the bottom views, H atoms have been omitted for clarity.

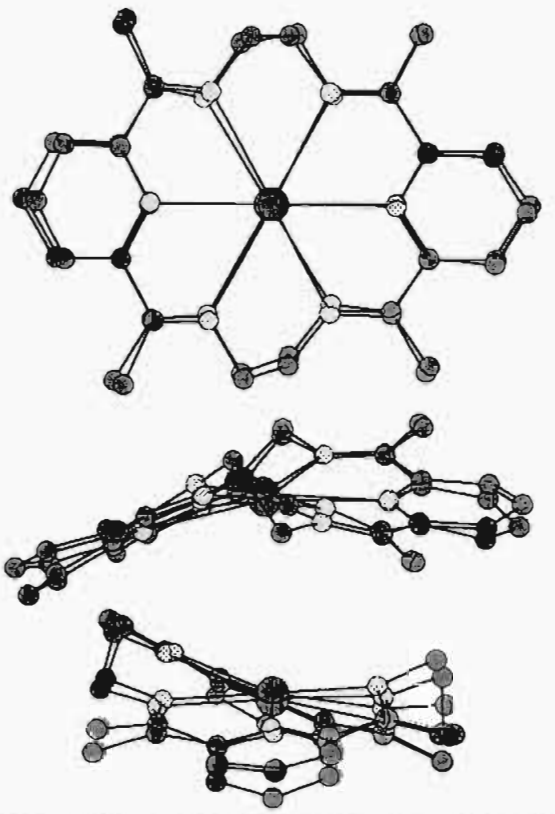

Figure 9. Overlays of the $[Gd(HAM)]^{3+}$ moiety in the MM-calculated structure and that obtained from the X-ray crystal structure of $[Gd(HAM)(acetate)_2]Cl\cdot 4H_2O$. H atoms have been omitted for clarity.

MM optimizations of Gd complexes of π-conjugated ligands like HAM, DAPSC, and texaphyrin take much longer (roughly an order of magnitude) due to the Hückel MO calculation. The following protocol was found to be useful in speeding up the optimization. First, the geometry is optimized with the HMO correction turned off. Test calculations on texaphyrin, HAM,

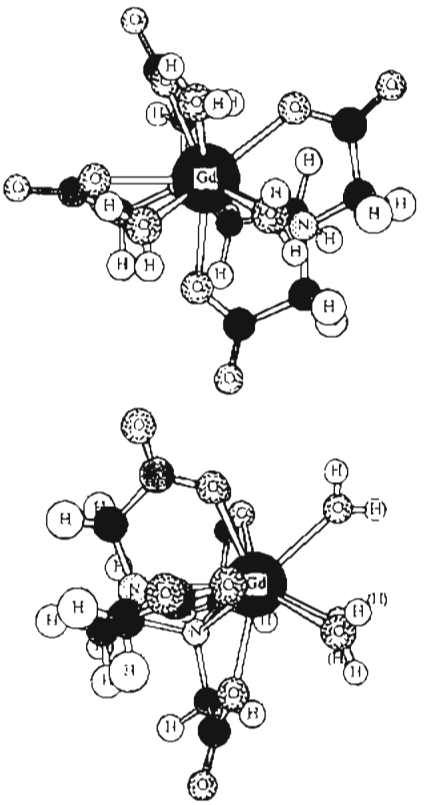

Figure 10. MM-optimized structure of $[Gd(EDTA)(OH_2)_3]^-$ viewed normal (top) and parallel (bottom) to the plane defined by the oxygen atoms of the aqua ligands.

and DAPSC complexes show minimal differences in geometry (even with respect to the tertiary structure of the conjugated ligand) with or without the π-conjugation correction. Second, the rough "nonconjugated" minimum energy geometry is used as a starting point for geometry optimization with the Hückel MO, π-conjugation correction included.

$[Gd(EDTA)(H_2O)_3]^-$, 8. Amino polycarboxylate ligands such as DTPA, DOTA (1,4,7,10-tetraazacyclododecane-*N*,*N*′,*N*″,*N*‴-tetraacetic acid), and their derivatives are prevalent in commercial Gd MRI contrast agents.[48] It is thus imperative to accurately model such ligand types. The agreement in bond lengths and bond angles between MM-optimized **8** (Figure 10) and X-ray diffraction data[49] for $[Gd(EDTA)(H_2O)_3]^-$ is excellent. The average differences in bond lengths between MM and X-ray data are 0.03 Å for all 28 bonds and 0.04 Å for nine Gd−L bonds, average differences of 2% and 3%, respectively. The average differences between MM and X-ray data are 2° for all 70 bond angles and 3° for 36 L−Gd−L bond angles, deviations of ≈2−3% in both cases. However, the average difference between torsions in the crystal and computed structure for $[Gd(EDTA)(H_2O)_3]^-$ is 11°. Although the differences could be explained by forces such as crystal packing, it was investigated more fully to understand the cause for the deviation. Upon comparison of MM and X-ray metric data for **8**, the largest deviations (as high as 37°) occur in two torsion types which entail rotation about O(coordinated carboxylate)−C(carbonyl) bonds: Gd• • •O−C=O and Gd• • •O−C−C (**E**). Analysis of the data suggests inappropriate modeling of these torsions for

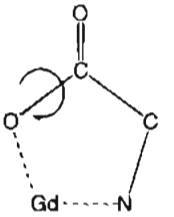

E

coordinated carboxylates. Although many Gd−X−Y−Z torsions have been set to zero, particularly if X−Y describes a single bond, we have been able to accurately model Gd complexes. Perhaps there is some multiple-bonding character in the O(coordinated carboxylate)−C(carbonyl) bond of the carboxylate moiety and hence a torsional barrier appreciably greater than zero. Thus, the force field was reanalyzed with emphasis on Gd• • •O−C=O and Gd• • •O−C−C torsional parameters.

We chose two simple models (the H−O−C=O torsional potential of a carboxylic acid and the C−O−C=O torsional potential of an ester), both of which have substantial 2-fold rotational barriers in the standard force field. Some researchers have used $C(sp^3)$−X−Y−Z torsional potentials to model metal−X−Y−Z torsions, and the present line of inquiry is consistent with these previous studies.[19b] Two test optimizations of **8** were carried out. First, $[Gd(EDTA)(H_2O)_3]^-$ was reoptimized (starting from the previous MM-optimized geometry) using the standard MM2 H−O−C=O potential to model Gd• • •O−C=O and Gd• • •O−C−C torsions; all other parameters remained unchanged. The results were similar to those described above. The second test, i.e. optimization of $[Gd(EDTA)(H_2O)_3]^-$ using the MM2 C−O−C=O potentials to model Gd• • •O−C=O and Gd• • •O−C−C, gave superior agreement with X-ray crystallographic data.[49] A statistical analysis of the torsions shows the average difference between crystallographic and molecular mechanics data to be 6°, or roughly half the original difference and similar in magnitude to that seen for previous test complexes. The average difference in bond lengths and bond angles for the latter parametrization are nearly equal to those seen for the original parametrization. Although it is likely that further refinement to the torsional parameters would yield improved agreement between theory and experiment, these calculations serve to highlight that careful attention must be paid to the details of the parametrization. An overlay of the calculated and X-ray structures of **8** is shown in Figure 11.

Summary and Conclusions

This paper describes the extension of an molecular mechanics force field for organic molecules to Gd(III) complexes. Complexes of Gd(III) are of interest in the context of magnetic resonance imaging contrast agent design. Several important conclusions were reached as a result of this research and are summarized below.

New MM atom types were developed to describe typical ligating types preferred by Ln(III) ions and hence prevalent in Gd(III) contrast agents. These atom types are neutral sp^3 nitrogen (amines), neutral sp^3 oxygen (ethers, alcohols, and waters), neutral sp^2 oxygen (carbonyl), neutral sp^2 nitrogen (imines and pyridines), and oxygen with a negative charge (carboxylates). A major assumption of this work is that metal-independent MM parameters are transferable from the metal-free ligand to the metal−ligand complex. The agreement found between calculated and predicted structures is proof of the validity of the transferability assumption for Gd(III) coordination complexes.

A very simple force field was used in order to minimize computational effort. Such an approach also serves to simplify

(48) (a) MAGNEVIST (a registered trademark of Berlex Industries) is gadopentetate dimeglumine, a derivative of GdDTPA. (b) ProHance (a registered trademark of Squibb Diagnostics) is gadoteridol, a derivative of GdDOTA. (c) OMNISCAN (a registered trademark of Sanofi Winthrop Pharmaceuticals) is gadodiamide, a derivative of GdDTPA.

(49) Templeton, L. K.; Templeton, D. H.; Zalkin, A.; Ruben, H. W. *Acta Crystallogr.* **1982**, *B38*, 2155−2159.

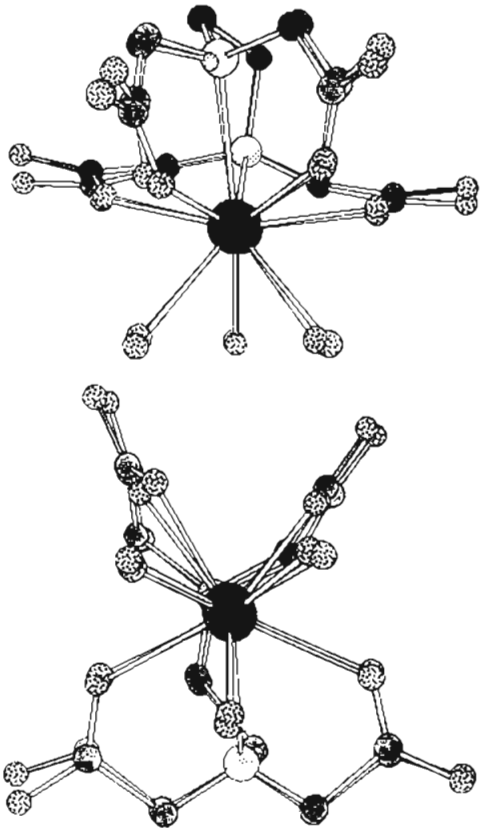

Figure 11. Overlays of MM-optimized and X-ray structures of $[Gd(EDTA)(OH_2)_3]^-$.

force field derivation and can be easily extended to related families of metallopharmaceuticals. No elaborations are used to calculate the contributions to U_{steric} in eq 1 such as higher order stretching and angle-bending terms, stretch−bend terms, etc. For the diverse ligand types studied, the newly derived molecular mechanics force field is able to predict bond lengths to within several hundredths of an angstrom and bond angles to within a few degrees of X-ray metric, differences of 1−3%. Torsions, which are the softest and hence most difficult to accurately model, are also accurately predicted. In general, MM-predicted torsions agree with experiment to within an average of 5−7°. Thus, the newly created parameters can be used to routinely study realistically-sized lanthanide complexes. The complexes discussed above contain between 40 and 70 atoms, considerably more than is feasible to consider using quantum chemical methods, and all calculations are carried out using standard computer platforms and software.[26]

The structural data obtained with the present force field can be used as a starting point for other computational methods used in drug design to yield complementary information and further assess potential Gd(III) MRI contrast agents. For example, given a minimized structure, one can estimate the strength of the Gd(III)−ligand interaction (an important determinant of complex stability and hence contrast agent toxicity) using molecular mechanics[22,23] or empirical approaches.[50] A combination of MM (for quick structural prediction) and quantum calculations[26−28] (at the MM-optimized geometry) can be used to probe electronic properties of a potential MRI contrast agent, for example, interaction of unpaired electrons on Gd(III) with inner/outer coordination sphere waters or hydrophobicity/hydrophilicity of the Gd(III)−ligand complex. The present force field could also be used in conjunction with molecular dynamics[51] to explore conformational space in cases where there are no experimental data to provide a starting structure. It should also be possible to use this force field to generate lead compounds for use in structure−activity analyses such as QSAR (quantitative structure activity relationship).[3]

Whatever the application or extension, the first step in any computer-aided drug design scenario is often accurate determination of the three-dimensional arrangement of the atoms in the drug. Development of reliable methods for quick structure prediction of biomedically significant metal complexes, using standard computer platforms and software, is an important first step in allowing the bench chemist to use computers to aid in the design of drugs containing elements from the entire periodic table.

Acknowledgment. This research was supported in part by a Faculty Research Grant from the University of Memphis and the U.S. Department of Energy (Grant DE-FG05-94ER14460 from Division of Chemical Sciences, Office of Basic Energy Sciences, Office of Energy Research). The authors also acknowledge the help of Vincent Lynch (University of Texas) and Robin Rogers (Northern Illinois University) in obtaining X-ray data for several Gd(III) complexes experimentally characterized in their laboratories.

Supporting Information Available: A complete tabulation comparing theoretical and experimental metric parameters for structures of the compounds discussed in the text (**1**, **2**, **4**, **6**, **7**, **8**) (22 pages). This material is contained in many libraries on microfiche, immediately follows this article in the microfilm version of the journal, and can be ordered from the ACS; see any current masthead page for ordering information.

IC950214V

(50) Carugo, O.; Bisi Castellini, C. *Inorg. Chim. Acta* **1992**, *191*, 115−120.
(51) Karplus, M.; McCammon, J. A. *Annu. Rev. Biochem.* **1983**, *52*, 263−300.